Hydration of the Calcium Dication: Direct Evidence for Second Shell Formation from Infrared Spectroscopy

Matthew F. Bush, Richard J. Saykally, and Evan R. Williams*[a]

Infrared laser action spectroscopy in a Fourier-transform ion cyclotron resonance mass spectrometer is used in conjunction with ab initio calculations to investigate doubly charged, hydrated clusters of calcium formed by electrospray ionization. Six water molecules coordinate directly to the calcium dication, whereas the seventh water molecule is incorporated into a second solvation shell. Spectral features indicate the presence of multiple structures of $Ca(H_2O)_7^{2+}$ in which outer-shell water molecules accept either one (single acceptor) or two (double acceptor) hydrogen bonds from inner-shell water molecules. Double-acceptor water molecules are predominately observed in the second solvent shells of clusters containing eight or nine water molecules. Increased hydration results in spectroscopic signatures consistent with additional second-shell water molecules, particularly the appearance of inner-shell water molecules that donate two hydrogen bonds (double donor) to the second solvent shell. This is the first reported use of infrared spectroscopy to investigate shell structure of a hydrated multiply charged cation in the gas phase and illustrates the effectiveness of this method to probe the structures of hydrated ions.

Introduction

Metal ions profoundly affect the local properties of water both through direct interactions and through more subtle indirect interactions with the hydrogen-bond network. These effects are the result of a delicate balance between cation–water interactions and the disruption of intrinsic solvent structure. One strategy to gain a detailed understanding of how ions and water molecules interact is to build up a solution, one molecule of water at a time.[1] Vibrational spectroscopy is a powerful structural tool for investigating hydrated ions, and has been used to investigate the structures of hydrated monovalent cations, including Ag^+,[2] H^+,[3–6] Cs^+,[7,8] Cu^+,[2] K^+,[9] Mg^+,[10] NH_4^+,[11,12] and Ni^+[13] and hydrated anions, including Cl^-,[14,15] e^-,[16] F^-,[15,17] HO^-,[18] and SO_4^{2-}.[19]

Despite serving critical regulatory and structural roles in biology, experimental studies of hydrated, multiply charged ions have lagged behind those of singly charged ions, owing to the great difficulty in producing them in significant abundances; for example, formation of doubly hydrated, divalent calcium by condensation results in rapid dissociation aided by Coulomb repulsion [Eq. (1)]:[20]

$$Ca^{2+}(H_2O) + H_2O \rightarrow [CaOH]^+ + H_3O^+ \qquad (1)$$
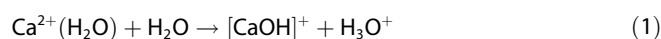
Charge-separation reactions of this type can prevent the formation of larger multiply charged clusters through water condensation. Electrospray ionization, which can form ions by evaporating water from more heavily hydrated clusters,[21] has enabled the study of a plethora of previously inaccessible, multiply charged ions, such as $Ca^{2+}(H_2O)_n$, $n \geq 2$.[22–31] Hydrated triply charged metal ions have only recently been observed and nanometer-sized droplets were required to prevent charge

reduction.[32] Hydrated doubly charged metal ions have been investigated using blackbody infrared radiative dissociation (BIRD),[28–30] collision-induced dissociation (CID),[23,33] electron-capture dissociation (ECD),[31,33] electronic spectroscopy,[34] guided ion-beam mass spectrometry (GIBMS),[25] high-pressure mass spectrometry (HPMS),[24,26] and ion/neutral chemistry,[22] whereas the characterization of hydrated triply charged metal ions is only just beginning.[32]

For divalent calcium, establishing the inner-shell coordination number (CN) of water has been the subject of numerous computational and experimental studies.[25,26,29,35–43] Binding energies of water to hydrated divalent calcium clusters in the gas phase have been measured by HPMS,[26] BIRD,[29,30] and GIBMS.[25] These values are in reasonable agreement with each other, density functional theory (DFT) calculations,[25,29,35] and recent MP2 calculations.[25] These results and sequential entropy measurements[26] indicate that the CN of divalent calcium is six,[26] although a heptacoordinated cluster was not explicitly ruled out.[29] Divalent calcium in bulk aqueous solution has been examined using many techniques including classical dynamics,[38,39] Car–Parrinello molecular dynamics,[37] hybrid QM/MM dynamics,[39,40] neutron diffraction,[41] X-ray diffraction,[42] and X-ray absorption fine-structure spectroscopy.[43] Many of these studies suggest that CN of this ion in bulk solution is greater than that in the gas phase, although reported solution values range from 5.5–10.[37–43]

[a] M. F. Bush, Prof. R. J. Saykally, Prof. E. R. Williams
Department of Chemistry, University of California
Berkeley, California 94720-1460 (USA)
Fax: (+1) 510-642-7714
E-mail: williams@cchem.berkeley.edu

Infrared spectroscopy is a powerful probe of CN for gaseous clusters because of the dramatic shifts in band frequencies between clusters in which all water molecules coordinate directly to the metal ion and those in which water molecules occupy positions in outer solvent shells; for example, the photodissociation spectrum of $Ni^+(H_2O)_3$ exhibits bands near 3620 and 3700 cm^{-1}, assigned to the nonbonded symmetric (v_{sym}) and asymmetric (v_{asym}) stretches of acceptor-only water molecules, whereas that of $Ni^+(H_2O)_4$ contains an additional band at 3180 cm^{-1}, assigned to the stretching mode of an inner-shell water molecule donating a hydrogen bond to a second-shell, single-acceptor water molecule.[13] These spectral signatures indicate that the first three water molecules directly solvate the metal ion, whereas the forth water molecule is incorporated into a second solvent shell,[13] that is, the CN of Ni^+ is three.

Here, infrared action spectra of $Ca^{2+}(H_2O)_n$, $n = 4$–10, are used to determine the CN and binding modes of water to divalent calcium. This is the first reported use of infrared spectroscopy to investigate multiply charged, hydrated cations in the gas phase.

Results and Discussion

General Features

Infrared photodissociation spectra for $Ca^{2+}(H_2O)_{4-10}$ are shown in Figure 1. Ion cell copper jacket temperatures are reported
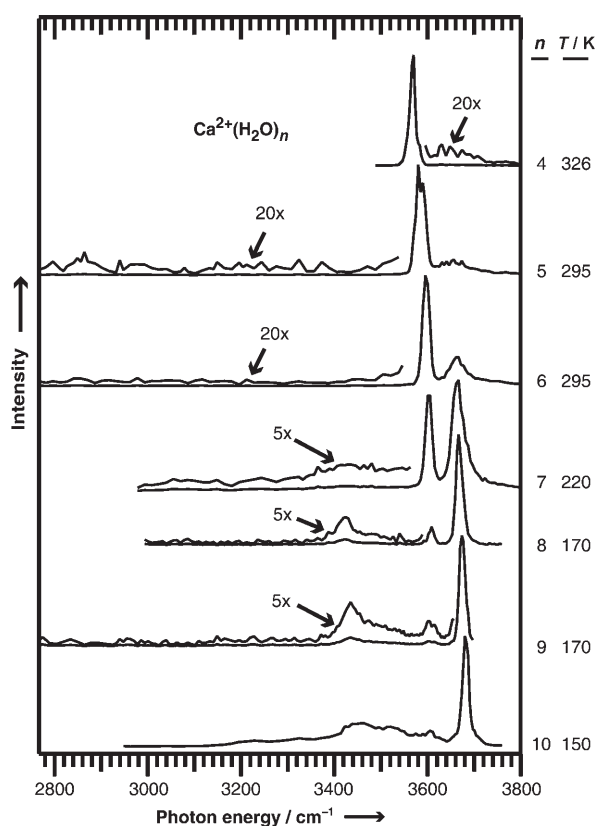

Figure 1. Photodissociation spectra of $Ca^{2+}(H_2O)_{4-10}$. Cluster identity (n) and copper jacket temperature (T) are labeled for each spectrum.

for each spectrum and were chosen to ensure that clusters are thermally stable over the timescale of the experiments, yet have enough internal energy to readily dissociate upon laser irradiation at frequencies at which the ions readily absorb. Higher temperatures were used for the smaller clusters because water is more tightly bound with decreasing cluster size.[25,26,29,30] Under these conditions, a substantial fraction of the population is within a single IR photon energy for the appearance of the loss of a water molecule from the larger clusters. Absorption of multiple photons by both the precursor and fragment ions can also occur. The sequential loss of up to four neutral water molecules was the only observed photodissociation pathway.

The spectra for the smallest clusters ($n = 4$–6) exhibit only two bands and are qualitatively similar to those reported previously for $Ag^+(H_2O)_3$,[2] $K^+(H_2O)_3$,[9] and $Ni^+(H_2O)_3$,[13] which adopt structures in which all water molecules coordinate directly with the metal ion. An isolated water molecule has high-frequency bands orginating at 3649 and 3731 cm^{-1}, corresponding to the symmetric (v_{sym}) and asymmetric (v_{asym}) stretch, respectively.[44] Singly hydrated metal ions also exhibit these two bands, but the frequencies are red-shifted compared to those of isolated water. This effect has been observed in clusters of H_3O^+ (3530 and 3514 cm^{-1} for v_{sym} and v_{asym}, respectively),[45] $Li^+(H_2O)\cdot Ar$ (3629 and 3691 cm^{-1}),[46] and $Ni^+(H_2O)\cdot Ar_2$ (3623 and 3696 cm^{-1}).[13] Duncan and co-workers have explained this red shift through partial electron transfer from the water molecule to the charge,[13] causing a frequency shift analogous to the extremely red-shifted v_{sym} and v_{asym} modes observed for $H_2O^{+\cdot}$ at 3213 and 3259 cm^{-1}, respectively.[47] For larger ions with low charge density, this effect can be very small: v_{sym} and v_{asym} for $Cs^+(H_2O)$ are 3636 and 3758 cm^{-1}, respectively.[7] The charge density of divalent calcium is very large and these bands for the smallest clusters are highly red-shifted relative to those for the isolated water molecule, consistent with the increased charge transfer to divalent metal ions relative to monovalent metal ions observed in bulk aqueous solution.[48]

No photodissociation was observed below 3520 cm^{-1} for $n = 4$–6. In contrast, photodissociation does occur in this region for $n = 7$–10. Many of these lower frequency bands observed for the larger clusters share similarities with those observed for $H^+(H_2O)_{n>2}$[4–6] and $Ni^+(H_2O)_{n>3}$,[13] which adopt structures with hydrogen bonding between water molecules. The observation of these bands for the larger clusters is indicative of structures in which additional water molecules no longer directly coordinate with the metal ion, but instead form a second solvent shell. This indicates that the coordination number (CN) of divalent calcium in these clusters is six.

The structures of $Ca^{2+}(H_2O)_{4-10}$, were also investigated with extensive conformational searching and ab initio calculations. Vibrational spectra calculated for these candidate structures can be compared to the photodissociation spectra to yield additional insights into the specific structures of these ions. Because the conformational spaces of these ions are extremely large, only the lowest-energy structures identified and those that illustrate important bonding motifs are presented. Addi-

tionally, there are the attendant uncertainties resulting from comparing absorbance spectra calculated at zero K using the double-harmonic approximation with experimental action spectra obtained at finite temperatures.

Ions with a Single Solvent Shell: $Ca^{2+}(H_2O)_{4-6}$

The photodissociation spectra of $Ca^{2+}(H_2O)_{4-6}$ are qualitatively similar and exhibit only two bands (Figures 2–4), assigned to the v_{sym} and v_{asym} modes of water. For $Ca^{2+}(H_2O)_4$, only one

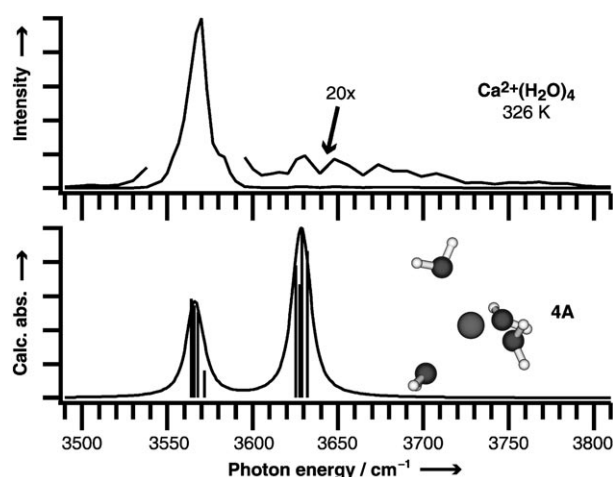**Figure 2.** Photodissociation spectrum of $Ca^{2+}(H_2O)_4$ obtained at a copper jacket temperature of 326 K and the spectrum for conformer **4 A** from B3LYP/LACVP $++$** calculations.

Figure 3. Photodissociation spectra of $Ca^{2+}(H_2O)_5$ obtained at copper jacket temperatures of 295 and 326 K and the spectra for three low-energy conformers (**5 A**–**5 C**) from B3LYP/LACVP $++$** calculations. Intensities of "stick" representations of nonbonded hydrogen stretches have been multiplied by five.

stable structure in which the water molecules are tetrahedrally coordinated with the metal ion (**4 A**, Figure 2) was identified. There is good agreement between the spectrum calculated for this structure and that obtained experimentally for v_{sym}, whereas v_{asym} in the photodissociation spectrum is very broad and of extremely low intensity. The bandwidth of the v_{asym} band is likely due to excited internal rotations in these ions. For water in C_{2v} point groups, v_{sym} is a parallel transition, allowed for $\Delta K = 0$, whereas v_{asym} is a perpendicular transition, allowed for $\Delta K = \pm 1$. Therefore, the v_{asym} band in this spectrum includes transitions originating from a distribution of K states, as discussed by Lee and co-workers for small protonated water clusters,[6] and Vaden et al. for $Li^+(H_2O)\cdot Ar$.[46]

The v_{asym} band of $Ca^{2+}(H_2O)_4$ is very weak relative to the v_{sym} band, consistent with the decreased relative intensity of this band exhibited in many other water-loss action spectra.[11] Niedner-Schatteburg and co-workers proposed that weak intramolecular vibrational relaxation (IVR) coupling for v_{asym} reduces the photodissociation efficiency for this mode for $NH_4^+(H_2O)$.[11] Although many of the effects of slow IVR should be significantly reduced in these experiments as a result of the 100 ms time period between laser pulses and the presence of multiple water molecules, radiative emission from v_{asym} should be fast and this may be a competitive relaxation mechanism.[49] Alternatively, the absorption of multiple photons is more important
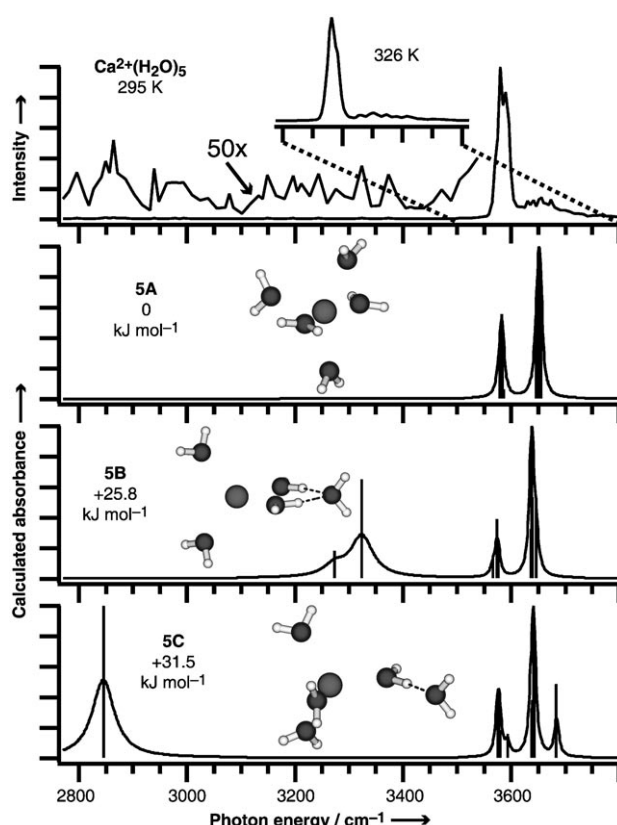
Figure 4. Photodissociation spectrum of $Ca^{2+}(H_2O)_6$ obtained at a copper jacket temperature of 295 K and the spectra for two low-energy conformers (**6 A**–**6 B**) from B3LYP/LACVP $++$** calculations. Intensities of "stick" representations of nonbonded hydrogen stretches have been multiplied by five.
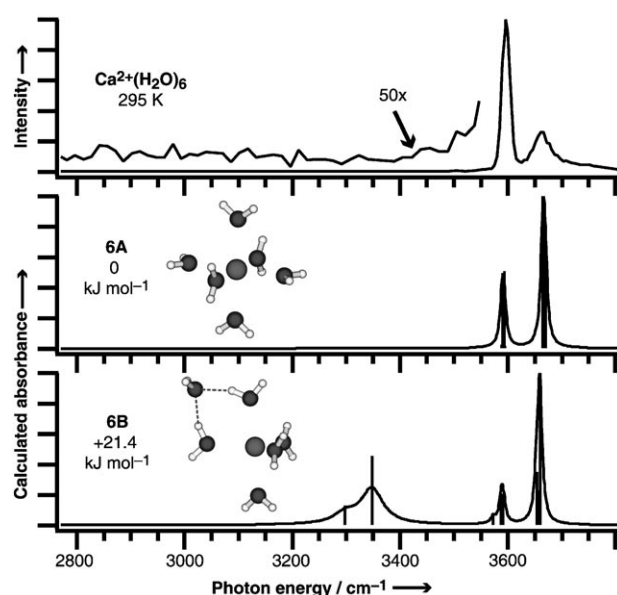
for the smaller clusters because of higher dissociation energies for the loss of a water molecule. This may lead to a nonlinear relationship between photodissociation efficiency and absorbance cross-section, consistent with the observed decrease in the v_{asym}/v_{sym} intensity ratio with increasing ligand binding energies.[11] If that is the case—particularly given that these bands have very different widths—the ratio of integrated photodissociation intensities for v_{asym} and v_{sym} would not equal that of the calculated oscillator strengths. Additionally, the K-state distribution of $Ca^{2+}(H_2O)_4$ ions that have absorbed a photon may strongly differ from that at equilibrium, thus decreasing the cross-section for the absorption of additional photons. The agreement between the relative intensities of the free-v_{sym} and free-v_{asym} photodissociation bands and those for the calculated oscillator intensities improves with increasing cluster size, consistent with decreasing dissociation energies for the loss of a water molecule and reduced K-sub-band structure for the larger clusters.

Multiple, energetically competitive candidate structures with a range of CN values were identified for all larger clusters. All five water molecules in the lowest-energy $Ca^{2+}(H_2O)_5$ structure coordinate directly to the metal ion in a distorted square pyramidal structure with partial trigonal bipyramidal character (**5A**, Figure 3). This structure has two classes of vibrational modes in the OH-stretch region: v_{sym} (3579–3586 cm^{-1}) and v_{asym} (3647–3655 cm^{-1}). Alternatively, $Ca^{2+}(H_2O)_5$ can adopt structures with a tetrahedral inner shell and in which the second-shell water molecule accepts two (**5B**, double acceptor) or one (**5C**, single acceptor) hydrogen bonds from the inner shell. The frequencies v_{sym} (3556–3579 cm^{-1}) and v_{asym} (3637–3643 cm^{-1}) for most of the acceptor-only water molecules in **5B** and **5C** are slightly red-shifted from those modes in **5A**, whereas those for the single-acceptor water molecule in **5C** are noticeably blue-shifted. The dangling-OH stretches for **5B** and **5C** (the stretching mode for the nonbonded hydrogen of a single-donor water molecule) are superimposed on the v_{asym} bands for the inner-shell, acceptor-only water molecules.

Although structures with second solvent shells have some similar bands to those of **5A**, the calculated spectra for **5B** and **5C** have additional bands at unique frequencies. The stretching modes for bonded hydrogen atoms are extremely red-shifted relative to their nonbonded counterparts. In **5B**, the two bonded hydrogen atoms couple to yield an intense mode where the two bonding hydrogen atoms oscillate in phase (3324 cm^{-1}) and a lower intensity mode where the oscillations are out of phase (3274 cm^{-1}). In **5C**, a single mode at 2845 cm^{-1} is calculated for the hydrogen-bond donor to the single-acceptor water molecule in the outer shell. However, **5C** has one negative frequency mode and attempts to locate a comparable local-minimum structure converged to **5B**. Although **5C** is not a local minimum at this level of theory, a related local-minima structure of $Ca^{2+}(H_2O)_6$ with a tetrahedral inner shell and both double- and single-acceptor water molecules in the second shell (not included, 52 kJ mol^{-1} higher in energy than **6A**) has a very similar donor stretch at 2898 cm^{-1}, thus indicating that **5C** provides reasonable insights into the hydrogen stretch band frequencies for such a structure.

Similar to $Ca^{2+}(H_2O)_{4–5}$, the lowest-energy structure of $Ca^{2+}(H_2O)_6$ is one in which all water molecules are in a single solvent shell (**6A**, Figure 4). The frequencies v_{sym} (3589–3595 cm^{-1}) and v_{asym} (3665–3669 cm^{-1}) for **6A** are slightly blue-shifted from the comparable modes in **5A**. The lowest-energy $Ca^{2+}(H_2O)_6$ structure with a CN of five has a trigonal bipyramidal inner shell and a double-acceptor water molecule in the outer shell (**6B**). The dangling-OH stretches and v_{asym} (3656–3661 cm^{-1}) and v_{sym} for the acceptor-only water molecules (3573–3592 cm^{-1}) have calculated band frequencies which are very similar to those of **5A**, whereas the bonded symmetric stretch modes (3298 and 3348 cm^{-1}) are blue-shifted by ≈ 24 cm^{-1} relative to the corresponding modes in **5B**. No stable structures with five-coordinate inner shells and a single-acceptor water molecule in the outer shell were identified; these clusters converged with structures **6A** or **6B** at this level of theory. Comparisons with **5C** and **7C** suggest that the bonded-hydrogen stretch of such a cluster would have a vibrational frequency of ≈ 3000 cm^{-1}, similar to the analogous modes calculated for a $Ca^{2+}(H_2O)_7$ structure with a five-coordinate inner shell and two single-acceptor water molecules in the outer shell (3008 cm^{-1}, not included, 33 kJ mol^{-1} higher in energy than **7B**). Structures with tetrahedral inner shells were explored, but are considerably higher in energy; for example, a structure with two double-acceptor outer-shell water molecules and D_{2d} symmetry is 36 kJ mol^{-1} higher in energy than **6A**.

Comparisons with spectra previously reported for other cationized water clusters and with spectra calculated here indicate that $Ca^{2+}(H_2O)_{4–6}$ all adopt structures in which the water molecules form a single solvent shell around the metal ion (**4A**, **5A**, and **6A**, respectively). The absence of any measurable bands in the 3000–3500 cm^{-1} region indicates that any populations of structures that have second-shell water molecules are exceedingly small. Alternatively, the absence of photodissociation at lower frequencies may be attributable to lower photodissociation efficiencies for these modes. Given the signal-to-noise of these spectra and the relatively small decrease in internal energy deposition for the slightly lower frequency photons, the photodissociation spectra for these clusters appear most consistent with structures containing a single solvent shell.

The v_{sym} and v_{asym} bands for $Ca^{2+}(H_2O)_n$ blue-shift with increasing hydration, which is consistent with increased charge solvation and reduced charge transfer from any given water molecule to the metal ion. Blue shifts, or reduced red shifts, of these bands with increasing hydration were observed by Lee and co-workers in small, protonated water clusters, $H^+(H_2O)_n$, $n = 1–3$,[6] and continue in the spectra of $H^+(H_2O)_n$, $n = 4–27$, reported by Miyazaki et al.[5] This phenomenon has also been observed in the spectra of $Ni^+(H_2O)_n$ with increasing n.[13] This trend is also consistent with the calculated band positions as a function of cluster size.

Onset of Second-Shell Formation

Many structures of $Ca^{2+}(H_2O)_7$ are calculated to be energetically competitive and are within 13 kJ mol⁻¹ of the lowest-energy structure, **7B**, in which the metal ion is octahedrally coordinated (CN = 6) and the remaining water molecule accepts two hydrogen bonds from single-donor water molecules in the inner shell (Figure 5). Breaking a single hydrogen bond (**7C**) costs
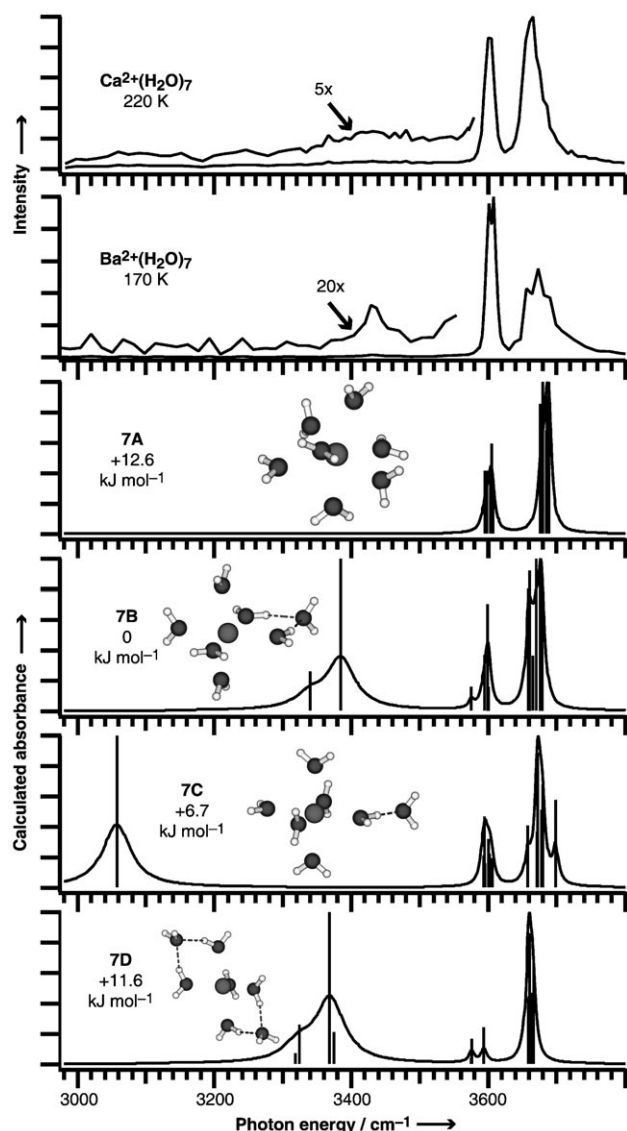

Figure 5. Photodissociation spectra of $Ca^{2+}(H_2O)_7$ and $Ba^{2+}(H_2O)_7$ obtained at a copper jacket temperatures of 220 and 170 K, respectively, and the spectra for four low-energy conformers (**7A–7D**) of $Ca^{2+}(H_2O)_7$ from B3LYP/LACVP++** calculations. Intensities of "stick" representations of nonbonded hydrogen stretches have been multiplied by five.

7 kJ mol⁻¹, which is remarkable, given that analogous structures of $Ca^{2+}(H_2O)_6$, wherein the second solvent shell contains one single-acceptor water molecule, were not found to be stable. Structures with all seven water molecules in the inner shell (**7A**,) or with two second-shell water molecules (**7D**) are

higher in energy—by only 13 and 12 kJ mol⁻¹, respectively—than **7B**.

Photodissociation from 3000–3500 cm⁻¹ occurs for $Ca^{2+}(H_2O)_7$, which indicates the presence of ions containing single- and double-acceptor water molecules in the outer shell. The photodissociation spectrum of this ion is well-explained by a superposition of the spectra calculated for structures **7B** and **7C**, although structures with different CN values may also be present and contribute to the photodissociation spectrum; for example, the calculated spectrum of **7D** (CN = 5) is very similar to that of **7B**, and is only 12 kJ mol⁻¹ higher in energy. The rather broad photodissociation exhibited by the inner-shell water molecules that donate hydrogen bonds to the second-shell water molecules suggests that the barrier between structures may be very small.

It is interesting to note that the relative photodissociation intensity observed below 3550 cm⁻¹ is significantly less than expected based on the calculated absorbance spectra for structures containing second-shell water molecules. This may be attributable to uncertainties in the calculated intensities, to reduced photodissociation efficiencies at lower frequencies, or to the presence of a significant population of structures with CN = 7.

The photodissociation spectrum of $Ba^{2+}(H_2O)_7$ provides an interesting comparison to that of $Ca^{2+}(H_2O)_7$. It has a very weak band at 3430 cm⁻¹, indicating the presence of a small population of ions with a structure analogous to **7B** of $Ca^{2+}(H_2O)_7$, but the photodissociation spectrum is consistent with the majority of the ions having a CN = 7. Higher photodissociation intensities at frequencies below ≈ 3550 cm⁻¹ suggest that a significantly greater fraction of the population of $Ca^{2+}(H_2O)_7$ has a CN ≤ 6 compared to that for $Ba^{2+}(H_2O)_7$. Additionally, the relative intensity of the free-v_{sym} band for $Ca^{2+}(H_2O)_7$ is substantially less than that exhibited by $Ba^{2+}(H_2O)_7$, consistent with hydrogen bonding between solvent shells depleting this high-frequency band in the former. These comparisons provide evidence that at least a significant fraction of the divalent calcium ions in the seven water-containing clusters are hexacoordinated, although quantitative comparisons between the relative abundances of the various structures is challenging.

Whereas bands corresponding to bonded-OH stretches are observed over a ≈ 500 cm⁻¹ range for $Ca^{2+}(H_2O)_7$, the photodissociation spectra for n = 8 and 9 exhibit a single broad feature for those stretches near 3430 cm⁻¹ and exhibited no photodissociation below 3350 cm⁻¹. The free-v_{sym} band for $Ca^{2+}(H_2O)_8$ is noticeably less intense relative to the free-v_{asym} band than that observed for $Ca^{2+}(H_2O)_7$, which is indicative of structures where the v_{sym} modes at high frequency are depleted as a result of the red-shifting of these modes for inner-shell water molecules involved in hydrogen bonding. When water molecules donate only a single hydrogen bond, the dangling-OH stretch lies at a frequency superimposed with v_{asym} for the acceptor-only water molecules in these clusters, whereas the bonded stretches occur at considerably lower frequency. This suggests that $Ca^{2+}(H_2O)_8$ has a smaller conformational space in which the second shell predominately consists of water molecules in double-acceptor positions (such as **8B**, Figure 6), in
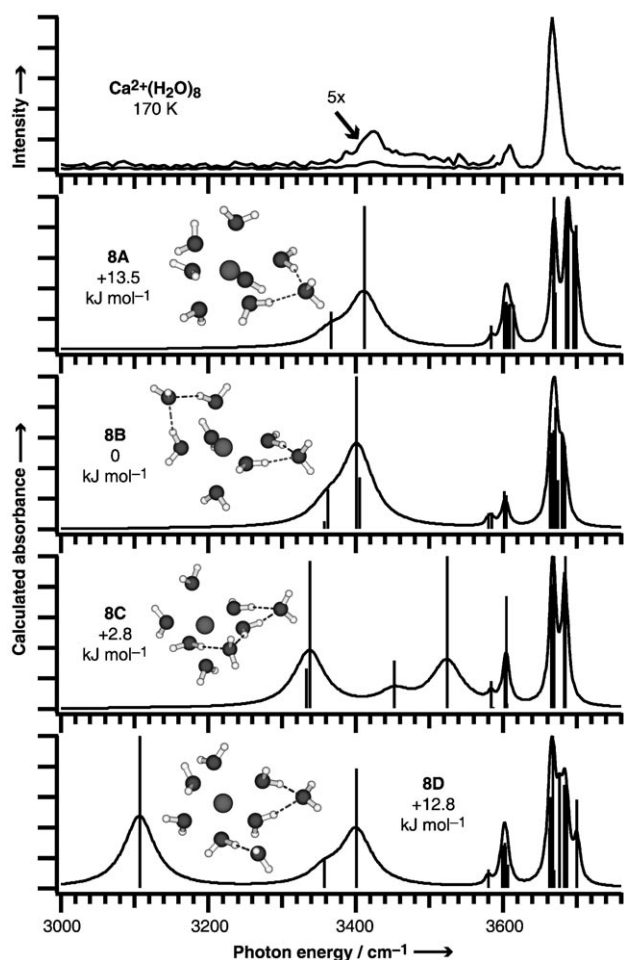
Figure 6. Photodissociation spectrum of $Ca^{2+}(H_2O)_8$ obtained at a copper jacket temperature of 170 K and the spectra for three low-energy conformers (**8A**–**8C**) from B3LYP/LACVP++** calculations. Intensities of "stick" representations of nonbonded hydrogen stretches have been multiplied by five.

Figure 7. Photodissociation spectrum of $Ca^{2+}(H_2O)_9$ obtained at a copper jacket temperature of 170 K and the spectra for four low-energy conformers (**9A**–**9D**) from B3LYP/LACVP++** calculations. Intensities of "stick" representations of nonbonded hydrogen stretches have been multiplied by five.

contrast to the mixture of single- and double-acceptor water molecules observed for $Ca^{2+}(H_2O)_7$.

The trends established for $Ca^{2+}(H_2O)_8$ extend to the photodissociation spectrum of $Ca^{2+}(H_2O)_9$. The spectrum for the larger cluster contains bands at very similar positions, although the free-υ_{sym} band is further depleted. This indicates that an octahedral inner shell, in which all water molecules donate a single hydrogen bond to double-acceptor water molecules in a second solvent shell (such as **9B**, Figure 7), continues to contribute significantly to these spectra. However, the bands near 3430 cm^{-1} in the photodissociation spectra of $Ca^{2+}(H_2O)_8$ and $Ca^{2+}(H_2O)_9$ are asymmetric and have increased intensity on the blue edge. Although these shoulders do not have resolved features, they are most consistent with populations of structures containing double-donor water molecules in the inner shell (**8C** and **9C**, respectively). The double-donor water molecule in **8C** (3 kJ mol^{-1} higher in energy than **8B**) has a υ_{sym} (3452 cm^{-1}) that is significantly blue-shifted relative to the donor stretch modes for the single-donor water molecules in **8B** (3334 and 3338 cm^{-1}), whereas υ_{asym} (3523 cm^{-1}) is significantly red-shifted relative to the dangling-OH stretch modes
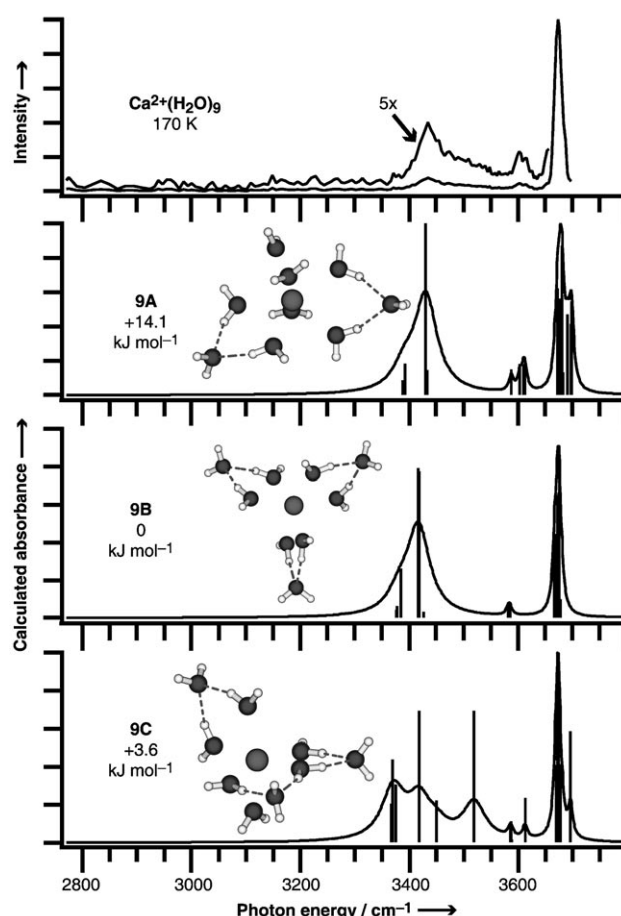
(3666 and 3667 cm^{-1}) in **8B**. These bands explain the photodissociation observed in this region, and these structures (**8C** and **9C**) are calculated to be very competitive in energy (+3 and +4 kJ mol^{-1} relative to **8B** and **9B**, respectively) and give insights into the spectral features characteristic of filling a second solvent shell, that is, when the majority of inner-shell water molecules donate two hydrogen bonds to the second solvent shell. Additionally, increased internal energy deposition at higher frequencies may increase the photodissociation efficiency and the relative intensity at the blue edges of bands in these action spectra.

Filling of the Second Solvent Shell

When $n=10$, it is no longer possible to have an octahedral inner shell consisting of water molecules that donate only a single hydrogen bond to acceptor-only water molecules, like those found computationally for the lowest-energy $Ca^{2+}(H_2O)_{7-9}$ structures. Low-energy structures with octahedral inner shells include those with double-donor water molecules in the inner shell (**10B**, 0 kJ mol^{-1}, see Figure 8), a single-acceptor water molecule in the second shell (**10D**, +5 kJ mol^{-1}) or third shell (**10C**, +1 kJ mol^{-1}), or hydrogen bonding be-
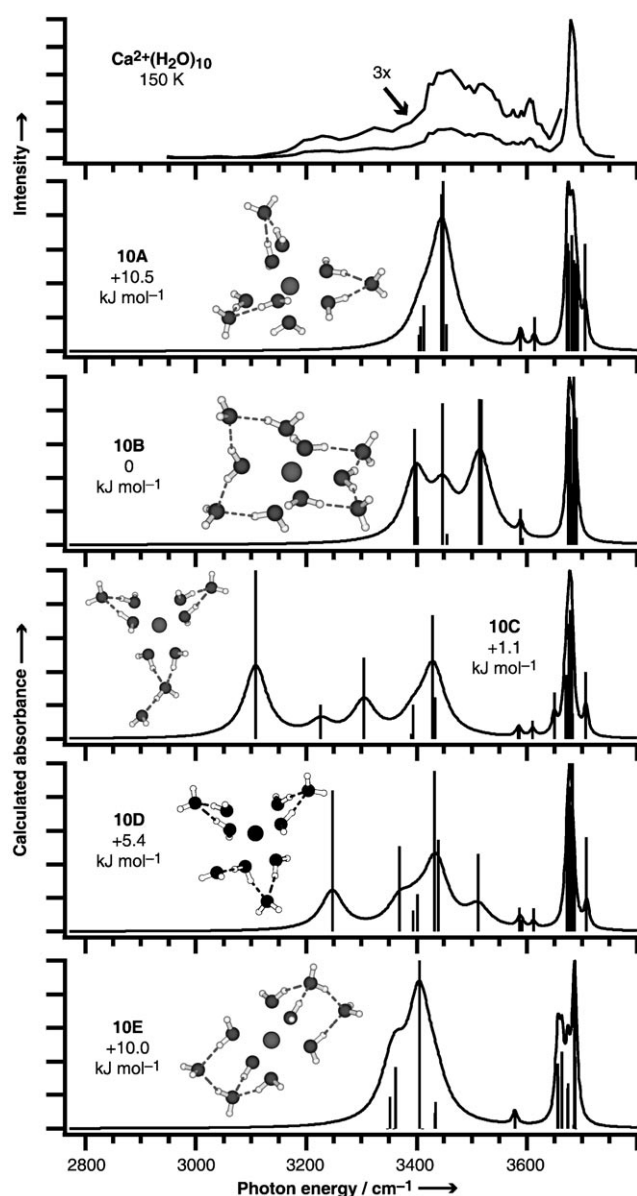
Figure 8. Photodissociation spectrum of $Ca^{2+}(H_2O)_{10}$ obtained at a copper jacket temperature of 150 K and the spectra for five low energy conformers (**10A**–**10E**) from B3LYP/LACVP++** calculations. Intensities of "stick" representations of nonbonded hydrogen stretches have been multiplied by five.

culated to be 4 kJ mol^{-1} lower in energy than **10D**, the single-acceptor water molecule in the former (3108 cm^{-1}) is calculated to be more strongly hydrogen bonded than that in the latter (3247 cm^{-1}), so the lack of measured intensity below 3150 cm^{-1} ostensibly limits the possibility that such a structure is present in these experiments. Also, the narrow bandwidth ($\approx$15 cm^{-1}) of the highest-frequency band in the experimental spectrum ($\approx$3680 cm^{-1}) precludes the presence of a large population of structures wherein the oscillators contributing in this region are spread out in frequency, such as **10E**, which has extensive intrashell hydrogen bonding. The data appear to be most consistent with a superposition of the spectra calculated for structures **10B** and **10D**, although it is likely that additional structures with similar hydrogen-bonding motifs also contribute to the observed photodissociation spectrum.

It is interesting to note that the relative photodissociation intensities exhibited below 3550 cm^{-1} by $Ca^{2+}(H_2O)_{10}$ are substantially greater than those for the smaller ions. The second solvent shell of $Ca^{2+}(H_2O)_{10}$ likely contains at least one additional water molecule than that of $Ca^{2+}(H_2O)_9$, although the difference in these values, perhaps four for the former and three for the latter, only partially explains the large increase in relative photodissociation intensities. Other factors that may contribute to this change with increasing cluster size are increased oscillator intensities for the new hydrogen bonding motifs identified for $Ca^{2+}(H_2O)_{10}$, depletion of the highest-frequency band due to the formation of additional double-donor water molecules, increased relative photodissociation efficiency at lower frequencies due to lower dissociation energies for the loss of a water molecule, or a greater increase in the ratio of second-shell water molecules.

Conclusions

Results from infrared action spectroscopy and supporting density functional theory calculations provide extensive insights into the solvation of the calcium dication. For clusters with up to six water molecules, there is no evidence for hydrogen bonding within the cluster and therefore all water molecules coordinate exclusively with the metal ion. Increasing the size of the cluster by one water molecule results in marked changes to the spectrum, resulting from the formation of a second solvation shell in which the seventh water molecule accepts either one or two hydrogen bonds from a six-coordinate inner shell. The addition of the eighth and ninth water molecules leads to structures with second shells consisting of water molecules predominantly accepting two hydrogen bonds from the inner shell. The addition of a tenth water molecule introduces structures with single-acceptor water molecules and increases the population of double-donor water molecules.

These results indicate the utility of infrared ion spectroscopy for establishing the coordination numbers of hydrated multiply charged ions. In addition, detailed information about how water in the second solvation shell interacts with the ions in the first shell can be obtained. By investigating still larger clusters and additional ions, it should be possible to obtain a more general understanding of ion solvation.

tween second-shell water molecules (**10E**, +10 kJ mol^{-1}). Structure **10A**, CN=7, is 11 kJ mol^{-1} higher in energy. Structures with CN=8 are at least 32 kJ mol^{-1} higher in energy (e.g. that with D_2 symmetry, not shown).

The new features in the photodissociation spectrum of $Ca^{2+}(H_2O)_{10}$ show how additional water molecules solvate the cluster. The broad absorbance near 3500 cm^{-1} indicates the presence of double-donor water molecules. The structures **10B** and **10D** have octahedral inner shells with double-donor water molecules and together provide good agreement with the experimental spectrum. The observed photodissociation below 3300 cm^{-1} is suggestive of structures containing single-acceptor water molecules, such as that in **10D**. Although **10C** is cal-

Experimental Section

Mass Spectrometry and Photodissociation: Experiments were performed on a Fourier-transform ion cyclotron resonance mass spectrometer with a 2.75 Tesla magnet.[50] Data were acquired using either an Odyssey data station prior to its ultimate demise (Finnigan-FTMS, Madison, WI) or subsequently with a "MIDAS"[51] modular FT/ICR data acquisition system. Nanospray ionization from a solution of $CaCl_2$ (1 mM, Fischer Scientific, Fair Lawn, NJ) in ultrapure water was used to form a distribution of $Ca^{2+}(H_2O)_n$ clusters. The abundance of the cluster of interest was optimized by changing conditions in the interface to the mass spectrometer.[32] Ions were accumulated and thermalized in a cylindrical ion cell[30] for 2–12 s with the assistance of dry N_2 gas ($\approx 10^{-6}$ Torr) introduced into the instrument through a piezoelectric pulsed valve. A mechanical shutter was subsequently closed to prevent additional ion accumulation and residual gases were pumped out for 4–10 s. Pressures $< 10^{-8}$ Torr were reached after ≈ 2 s and ions radiatively equilibrate with the surrounding instrument.[49,52] Ion cell temperatures, measured with a thermocouple attached directly to the copper jacket surrounding the cell, were controlled by cooling the copper jacket with a regulated flow of liquid nitrogen[30] or resistively heating the vacuum chamber.[52] Temperatures were equilibrated for at least 8 h prior to all experiments.

After isolating ions by using a stored-waveform inverse Fourier transform, the clusters were irradiated using tunable infrared light produced by an optical parametric oscillator/amplifier (OPO/OPA) system (LaserVision, Bellevue, WA) pumped by the fundamental of an Nd:YAG laser (≈ 8 ns pulses generated at a 10 Hz repetition rate, yielding ≈ 3.8 W, Continuum Surelight I-10, Santa Clara, CA). The idler component of the OPA (90–210 mW, ≈ 3 cm^{-1} bandwidth) was isolated using Brewster-angle-mounted silicon plates and aligned with the ions using a series of protected silver mirrors enclosed in a positive-pressure, dry nitrogen purge box containing calcium sulphate desiccant (W.A. Hammond Drierite Co. Ltd., Xenia, OH). Spectra for $Ca^{2+}(H_2O)_{4-6}$ were obtained using a 1 m CaF_2 spherical focusing lens placed ≈ 75 cm from the center of the ion cell; all remaining data were acquired using the unfocused output of the OPO/OPA. Light enters the vacuum chamber through a Brewster-angle-mounted CaF_2 window. Laser irradiation times were varied from 2–120 s to improve the signal-to-noise and dynamic range.

A mass spectrum was collected immediately after laser irradiation. Multiple experiments indicate that the observed photodissociation rate is first order, consistent with results from McLafferty and co-workers.[53] Infrared action spectra were obtained by plotting intensity as a function of laser frequency:[50]

$$\text{Intensity} = \ln \left\{ \left(\frac{[\text{Precursor\_Ion}]}{[\text{Precursor\_Ion}] + [\text{Fragment\_Ion}]} \right) \Big/ \text{time*power}(v) \right\} \qquad (2)$$

This yields a first-order photodissociation rate constant, normalized for laser power (s^{-1}W^{-1}). This enables results from experiments with different irradiation times to be integrated into a single infrared spectrum, and no smoothing or other manipulation of the spectral data was performed. No observable BIRD[52,54] occurred during these experiments, so no background correction to the data was required.

Computational Chemistry: Candidate low-energy structures were determined using conformational searching and chemical intuition. Initial structures were generated using Monte Carlo conformation searching with the MMFF94 force field as implemented in Macro-

model 8.1 (Schrödinger, Inc. Portland, OR). No constraints were placed on the initial structures and at least 10 000 conformations were generated. In these searches, the significant hydrogen bonding motifs were identified within the first several thousand conformations generated. Additional structures were obtained by adding or removing water molecules from the initial set of structures.

Candidate structures were energy-minimized with hybrid-method density functional calculations (B3LYP) using the LACVP* and LACVP++** basis sets as implemented in Jaguar v. 6.5 (Schrödinger, Inc., Portland, OR). Vibrational frequencies and intensities were calculated using numerical derivatives of the LACVP++** energy-minimized Hessian. Energies are from B3LYP/LACVP++** calculations, include zero-point energy corrections, and are reported relative to the global minimum structure. All vibrational frequencies have been scaled by 0.95. This scaling factor provides good agreement with photodissociation spectra in the free-OH region and is the same factor used previously for cationized arginine.[50] To approximate some of the temperature effects in the photodissociation spectra, line spectra are convoluted using 10 cm^{-1} FWHM (full width at half maximum) Lorentzian distributions for the nonbonded stretches and 50 cm^{-1} for the bonded stretches. Except where noted, all the structures yielded positive frequency vibrational modes, which is indicative of local-minima structures.

[1] A. J. Huneycutt, R. J. Saykally, *Science* **2003**, *299*, 1329–1330.
[2] T. Iino, K. Ohashi, K. Inoue, K. Judai, N. Nishi, H. Sekiya, *J. Chem. Phys.* **2007**, *126*, 194302.
[3] a) T. D. Fridgen, T. B. McMahon, L. MacAleese, J. Lemaire, P. Maître, *J. Phys. Chem. A* **2004**, *108*, 9008–9010; b) K. R. Asmis, N. L. Pivonka, G. Santambrogio, M. Brümmer, C. Kaposta, D. M. Neumark, L. Wöste, *Science* **2003**, *299*, 1375–1377; c) H. C. Chang, C. C. Wu, J. L. Kuo, *Int. Rev. Phys. Chem.* **2005**, *24*, 553–578.
[4] J. W. Shin, N. I. Hammer, E. G. Diken, M. A. Johnson, R. S. Walters, T. D. Jaeger, M. A. Duncan, R. A. Christie, K. D. Jordan, *Science* **2004**, *304*, 1137–1140.
[5] M. Miyazaki, A. Fujii, T. Ebata, N. Mikami, *Science* **2004**, *304*, 1134–1137.
[6] L. I. Yeh, M. Okumura, J. D. Myers, J. M. Price, Y. T. Lee, *J. Chem. Phys.* **1989**, *91*, 7319–7330.
[7] C. J. Weinheimer, J. M. Lisy, *J. Chem. Phys.* **1996**, *105*, 2938–2941.
[8] M. Kolaski, H. M. Lee, Y. C. Choi, K. S. Kim, P. Tarakeshwar, D. J. Miller, J. M. Lisy, *J. Chem. Phys.* **2007**, *126*, 074302.
[9] D. J. Miller, J. M. Lisy, *J. Chem. Phys.* **2006**, *124*, 024319.
[10] Y. Inokuchi, K. Ohshimo, F. Misaizu, N. Nishi, *J. Phys. Chem. A* **2004**, *108*, 5034–5040.
[11] T. Pankewitz, A. Lagutschenkov, G. Niedner-Schatteburg, S. S. Xantheas, Y. T. Lee, *J. Chem. Phys.* **2007**, *126*, 074307.
[12] a) Y. S. Wang, H. C. Chang, J. C. Jiang, S. H. Lin, Y. T. Lee, *J. Am. Chem. Soc.* **1998**, *120*, 8777–8788; b) E. G. Diken, N. I. Hammer, M. A. Johnson, R. A. Christie, K. D. Jordan, *J. Chem. Phys.* **2005**, *123*, 164309; c) H. C. Chang, Y. S. Wang, Y. T. Lee, *Int. J. Mass Spectrom.* **1998**, *180*, 91–102.

[13] R. S. Walters, E. D. Pillai, M. A. Duncan, *J. Am. Chem. Soc.* **2005**, *127*, 16599–16610.

[14] J. H. Choi, K. T. Kuwata, Y. B. Cao, M. Okumura, *J. Phys. Chem. A* **1998**, *102*, 503–507.

[15] W. H. Robertson, M. A. Johnson, *Annu. Rev. Phys. Chem.* **2003**, *54*, 173–213.

[16] a) N. I. Hammer, J. R. Roscioli, J. C. Bopp, J. M. Headrick, M. A. Johnson, *J. Chem. Phys.* **2005**, *123*, 244311; b) K. R. Asmis, G. Santambrogio, J. Zhou, E. Garand, J. Headrick, D. Goebbert, M. A. Johnson, D. M. Neumark, *J. Chem. Phys.* **2007**, *126*, 191105; c) J. R. Roscioli, N. I. Hammer, M. A. Johnson, *J. Phys. Chem. A* **2006**, *110*, 7517–7520.

[17] O. M. Cabarcos, C. J. Weinheimer, S. S. Xantheas, J. M. Lisy, *J. Chem. Phys.* **1999**, *110*, 5–8.

[18] a) C. Chaudhuri, Y. S. Wang, J. C. Jiang, Y. T. Lee, H. C. Chang, G. Niedner-Schatteburg, *Mol. Phys.* **2001**, *99*, 1161–1173; b) W. H. Robertson, E. G. Diken, E. A. Price, J. W. Shin, M. A. Johnson, *Science* **2003**, *299*, 1367–1372.

[19] a) J. Zhou, G. Santambrogio, M. Brümmer, D. T. Moore, L. Wöste, G. Meijer, D. M. Neumark, K. R. Asmis, *J. Chem. Phys.* **2006**, *125*, 111102; b) M. F. Bush, R. J. Saykally, E. R. Williams, *J. Am. Chem. Soc.* **2007**, *129*, 2220–2221.

[20] a) K. G. Spears, F. C. Fehnsenfeld, *J. Chem. Phys.* **1972**, *56*, 5698–5705; b) M. Beyer, E. R. Williams, V. E. Bondybey, *J. Am. Chem. Soc.* **1999**, *121*, 1565–1573.

[21] S. E. Rodriguez-Cruz, J. S. Klassen, E. R. Williams, *J. Am. Soc. Mass Spectrom.* **1999**, *10*, 958–968.

[22] S. E. Rodriguez-Cruz, E. R. Williams, *J. Am. Soc. Mass Spectrom.* **2001**, *12*, 250–257.

[23] A. A. Shvartsburg, K. W. M. Siu, *J. Am. Chem. Soc.* **2001**, *123*, 10071–10075.

[24] a) A. T. Blades, P. Jayaweera, M. G. Ikonomou, P. Kebarle, *Int. J. Mass Spectrom. Ion Processes* **1990**, *102*, 251–267; b) A. T. Blades, P. Jayaweera, M. G. Ikonomou, P. Kebarle, *J. Chem. Phys.* **1990**, *92*, 5900–5906.

[25] D. R. Carl, R. M. Moision, P. B. Armentrout, *Int. J. Mass Spectrom.* **2007**, *265*, 308–325.

[26] M. Peschke, A. T. Blades, P. Kebarle, *J. Phys. Chem. A* **1998**, *102*, 9978–9985.

[27] M. Peschke, A. T. Blades, P. Kebarle, *Int. J. Mass Spectrom.* **1999**, *187*, 685–699.

[28] a) S. E. Rodriguez-Cruz, R. A. Jockusch, E. R. Williams, *J. Am. Chem. Soc.* **1998**, *120*, 5842–5843; b) S. E. Rodriguez-Cruz, R. A. Jockusch, E. R. Williams, *J. Am. Chem. Soc.* **1999**, *121*, 1986–1987.

[29] S. E. Rodriguez-Cruz, R. A. Jockusch, E. R. Williams, *J. Am. Chem. Soc.* **1999**, *121*, 8898–8906.

[30] R. L. Wong, K. Paech, E. R. Williams, *Int. J. Mass Spectrom.* **2004**, *232*, 59–66.

[31] a) R. D. Leib, W. A. Donald, M. F. Bush, J. T. O'Brien, E. R. Williams, *J. Am. Chem. Soc.* **2007**, *129*, 4894–4895; b) R. D. Leib, W. A. Donald, M. F. Bush, J. T. O'Brien, E. R. Williams, *J. Am. Soc. Mass Spectrom.* **2007**, *18*, 1217–1231.

[32] M. F. Bush, R. J. Saykally, E. R. Williams, *Int. J. Mass Spectrom.* **2006**, *253*, 256–262.

[33] B. J. Duncombe, K. Duale, A. Buchanan-Smith, A. J. Stace, *J. Phys. Chem. A* **2007**, *111*, 5158–5165.

[34] K. P. Faherty, C. J. Thompson, F. Aguirre, J. Michne, R. B. Metz, *J. Phys. Chem. A* **2001**, *105*, 10054–10059.

[35] M. Pavlov, P. E. M. Siegbahn, M. Sandstrom, *J. Phys. Chem. A* **1998**, *102*, 219–228.

[36] A. K. Katz, J. P. Glusker, S. A. Beebe, C. W. Bock, *J. Am. Chem. Soc.* **1996**, *118*, 5752–5763.

[37] M. M. Naor, K. Van Nostrand, C. Dellago, *Chem. Phys. Lett.* **2003**, *369*, 159–164.

[38] a) M. M. Probst, T. Radnai, K. Heinzinger, P. Bopp, B. M. Rode, *J. Phys. Chem.* **1985**, *89*, 753–759; b) D. G. Bounds, *Mol. Phys.* **1985**, *54*, 1335–1355; c) G. Palinkas, K. Heinzinger, *Chem. Phys. Lett.* **1986**, *126*, 251–254; d) S. Obst, H. Bradaczek, *J. Phys. Chem.* **1996**, *100*, 15677–15687; e) S. G. Kalko, G. Sese, J. A. Padro, *J. Chem. Phys.* **1996**, *104*, 9578–9585.

[39] C. F. Schwenk, H. H. Loeffler, B. M. Rode, *J. Chem. Phys.* **2001**, *115*, 10808–10813.

[40] A. Tongraar, K. R. Liedl, B. M. Rode, *J. Phys. Chem. A* **1997**, *101*, 6299–6309.

[41] a) S. Cummings, J. E. Enderby, R. A. Howe, *J. Phys. C* **1980**, *13*, 1–8; b) N. A. Hewish, G. W. Neilson, J. E. Enderby, *Nature* **1982**, *297*, 138–139; c) Y. S. Badyal, A. C. Barnes, G. J. Cuello, J. M. Simonson, *J. Phys. Chem. A* **2004**, *108*, 11819–11827.

[42] a) T. Yamaguchi, S. Hayashi, H. Ohtaki, *Inorg. Chem.* **1989**, *28*, 2434–2439; b) G. Licheri, G. Piccaluga, G. Pinna, *J. Chem. Phys.* **1976**, *64*, 2437–2441; c) T. Megyes, T. Grosz, T. Radnai, I. Bako, G. Palinkas, *J. Phys. Chem. A* **2004**, *108*, 7261–7271.

[43] J. L. Fulton, S. M. Heald, Y. S. Badyal, J. M. Simonson, *J. Phys. Chem. A* **2003**, *107*, 4688–4696.

[44] G. Herzberg, *Molecular Spectra and Molecular Structure II. Infrared and Raman Spectra of Polyatomic Molecules*, Van Nostrand, New York, **1945**, pp. 280–282.

[45] M. H. Begemann, C. S. Gudeman, J. Pfaff, R. J. Saykally, *Phys. Rev. Lett.* **1983**, *51*, 554–557.

[46] T. D. Vaden, J. M. Lisy, P. D. Carnegie, E. D. Pillai, M. A. Duncan, *Phys. Chem. Chem. Phys.* **2006**, *8*, 3078–3082.

[47] T. R. Huet, C. J. Pursell, W. C. Ho, B. M. Dinelli, T. Oka, *J. Chem. Phys.* **1992**, *97*, 5977–5987.

[48] C. D. Cappa, J. D. Smith, B. M. Messer, R. C. Cohen, R. J. Saykally, *J. Phys. Chem. B* **2006**, *110*, 5301–5309.

[49] R. C. Dunbar, *Mass Spectrom. Rev.* **1992**, *11*, 309–339.

[50] M. F. Bush, J. T. O'Brien, J. S. Prell, R. J. Saykally, E. R Williams, *J. Am. Chem. Soc.* **2007**, *129*, 1612–1622.

[51] M. W. Senko, J. D. Canterbury, S. H. Guan, A. G. Marshall, *Rapid Commun. Mass Spectrom.* **1996**, *10*, 1839–1844.

[52] a) W. D. Price, P. D. Schnier, E. R. Williams, *Anal. Chem.* **1996**, *68*, 859–866; b) W. D. Price, P. D. Schnier, R. A. Jockusch, E. F. Strittmatter, E. R. Williams, *J. Am. Chem. Soc.* **1996**, *118*, 10640–10644.

[53] H. B. Oh, C. Lin, H. Y. Hwang, H. L. Zhai, K. Breuker, V. Zabrouskov, B. K. Carpenter, F. W. McLafferty, *J. Am. Chem. Soc.* **2005**, *127*, 4076–4083.

[54] a) R. C. Dunbar, T. B. McMahon, *Science* **1998**, *279*, 194–197; b) R. C. Dunbar, *Mass Spectrom. Rev.* **2004**, *23*, 127–158.